Nebrida
Journal of Electrical Systems and Inf Technol (2024) 11:8
https://doi.org/10.1186/s43067-024-00134-4

Journal of Electrical Systems and Information Technology

RESEARCH Open Access

Characterization of resonant coupled inductor in a wireless power transfer system

Alan P. Nebrida[1*]

*Correspondence:
ap_nebrida@nvsu.edu.ph

[1] Department of Electrical Engineering, Nueva Vizcaya State University, 3702 Bambang, Nueva Vizcaya, Philippines

Abstract

Wireless power transfer (WPT) has garnered significant interest as a potentially transformative technology in the energy sector, as it presents a novel approach to powering and charging devices. The functionality of this technology is predicated upon the utilization of electromagnetic coupling to facilitate the wireless transmission of energy between two entities. Despite the considerable potential, wireless power transfer (WPT) faces significant obstacles that restrict its practical feasibility. One notable challenge that arises is the decrease in power transfer efficiency as the distance between the transmitter and receiver increases. Moreover, the wireless power transfer (WPT) technology is further limited by its reliance on accurate alignment between the transmitting source and the receiving device, thereby posing challenges for its practical implementation. The issues present substantial obstacles to the widespread commercialization of wireless power transfer (WPT). This study seeks to improve the efficacy of power transfer by optimizing the resonance frequency of the power transfer in response to the challenges. By systematically manipulating various parameters including coil dimensions, input voltage levels, and operational frequency, a novel approach is proposed to enhance the efficiency of power transfer. The study additionally offers valuable insights regarding the correlation between the distance separating the coils and the efficiency of power transfer. The findings of this study offer a thorough empirical analysis and are supported by a strong theoretical framework, resulting in a substantial coefficient of determination ($R^2 = 0.937118$). This finding suggests that the linear regression model under consideration could account for approximately 93.7118 percent of the variability observed in the distance. The findings of this study establish a pathway toward enhanced and feasible wireless power technology, thereby establishing a robust basis for the prospective commercial implementation of wireless power transfer (WPT) systems.

Keywords: Wireless power transfer, Coupled magnetic resonance, Resonance frequency, Inductive coupling

Introduction

In today's world, there has been a notable surge in the production and enhancement of portable electronic devices, including mobile phones, laptops, and various other electronics and communication devices. Irrespective of their wireless communication capabilities, these devices necessitate periodic charging, typically accomplished by connecting them to a power source via a wall outlet. This phenomenon amplifies the pursuit

of novel methodologies aimed at enabling wireless power transmission to enhance the portability and mobility of such devices for end-users.

Wireless energy transfer, also known as wireless power transfer (WPT), refers to the transmission of electrical energy from a power source to an electrical load without the use of physical wires for interconnection. Various physiological techniques, such as laser technology, the piezoelectric principle, radio waves, microwaves, inductive coupling, and strong electromagnetic resonance, have been employed thus far for the purpose of wireless energy transfer. The utilization of a magnetic field for the transmission of substantial quantities of power ultimately gives rise to dissatisfaction and potential health hazards for individuals. The efficacy of the technique is notable; however, it is accompanied by a limitation due to its reliance on an unobstructed line of sight and the potential for harm to living organisms stemming from its underlying mechanism. Wireless energy transfer through the utilization of electromagnetic resonance phenomena has emerged as a viable option, particularly for short distances, owing to its notable attributes such as high-power transfer efficiency and absence of adverse impacts on human health according to the study conducted by Karalis et al. [9].

The technologies of wireless power transfer (WPT), electromagnetic induction, and microwave power transfer have gained significant recognition in academic and scientific fields. Nevertheless, the concept of electromagnetic resonance couplings has only emerged in recent times. The wireless power transfer technology necessitates the incorporation of three primary components: substantial air gaps, optimal efficiency, and a significant power output. Electromagnetic resonance coupling represents the sole technological approach that addresses the three elements.

The primary aim of this study is to provide a comprehensive characterization of resonant coupled inductors utilized in wireless power transfer systems. The primary objectives of this study are as follows: (1) to devise a wireless power transfer system; (2) to construct a model of the wireless power transfer system and execute simulations; (3) to ascertain the maximum distance over which the model can transmit power effectively, considering various orientations of the power transmitter; (4) to compare the outcomes of the simulations with empirically measured values; and (5) to formulate a systematic approach for analyzing data and establishing a methodology for characterizing wireless power transmission systems.

In contemporary times, engineers and designers engaged in the advancement of household devices are required to offer consumers an enhanced degree of convenience and adaptability. The investigation focused on a wireless power transfer (WPT) system as a potential solution for addressing the inconvenience associated with the utilization of a power cable. The utilization of wireless transmission proves advantageous in situations where the installation of interconnecting wires is impractical, poses risks, or is unfeasible. The attainment of wireless power transfer will enhance the portability and mobility of electronic devices by significantly improving the convenience of the charging process, eliminating the need for cord insertion into a socket. Furthermore, in the context of wireless charging, the safety of the charging process is enhanced by mitigating the risk of electric shock resulting from the deterioration of an aged cord.

The present study employs resonant inductive coupling as a means of wireless power transfer. The research study employs a low-power supply for the purpose of power

transmission. The study's focus is confined to the development of a simplified wireless power transfer (WPT) system utilizing a resonant coupled inductor configuration. This study encompasses several components, namely, the matching sections, the derivation of the relationship between the coupling coefficient and distance, and the examination of various parameters such as the quality factor, coupling coefficients, mutual inductance, and resonance frequency of the resonators. To facilitate the discernment of the system's operational status, the investigator employs a 12 V, 5W CYD LED bulb as the designated load. This study will not encompass alternative approaches for enhancing the efficacy of wireless power.

Methodology

The researcher used a systematic and comprehensive approach in this study on wireless power transfer (WPT) systems to investigate and substantiate the innovative contributions. The systematic depiction of this technique is shown in Fig. 1, Methodology Flow Chart, which outlines the consecutive stages that were done. The researcher first prioritized the gathering and analysis of data, which is a pivotal phase in which specifications for the hardware and software components of the wireless power transfer (WPT) system were established. The aforementioned stage had a crucial role in matching the specified criteria with the key goals, which included the creation of a refined frequency adjustment algorithm and the improvement of the overall efficiency of the system.

During the design process, the researcher carefully deliberated on the hardware and software components of the system. During this stage, the researchers developed a conceptual framework and conducted a material selection process for the hardware. The chosen materials were specifically targeted to facilitate the achievement of two objectives: increasing power transmission distances and integrating advanced materials to enhance overall performance. Concurrently, the algorithms, program flows, and software types required for the implementation of the software component were devised, with a particular emphasis on assuring stability and safety.

After the completion of the design phase, the project progressed to the assembly stage, during which the researcher diligently manufactured and integrated both hardware and software components. The aforementioned stage played a crucial role in the integration of the recently created algorithm and approaches aimed at improving efficiency. Thorough testing and debugging procedures were undertaken, resulting in crucial improvements that guaranteed the system's optimum functionality, with particular emphasis on efficiency at diverse distances and compatibility with a range of materials.

Subsequently, a sequence of studies was conducted, focusing on crucial factors such coil spacing, resonance frequency, voltage gain, and overall system efficiency. The purpose of these studies was to evaluate the effectiveness of novel methods in increasing the distance over which power can be transferred and improving the efficiency of the system by integrating sophisticated materials.

The ultimate phase included the determination of the parameters of the resonant coupled inductor in the wireless power transfer (WPT) system, principally obtained from the experimental inquiries. During this crucial stage, the researcher was able to evaluate the effectiveness of the unique contributions, which included the creation of an enhanced frequency adjustment algorithm and approaches aimed at enhancing

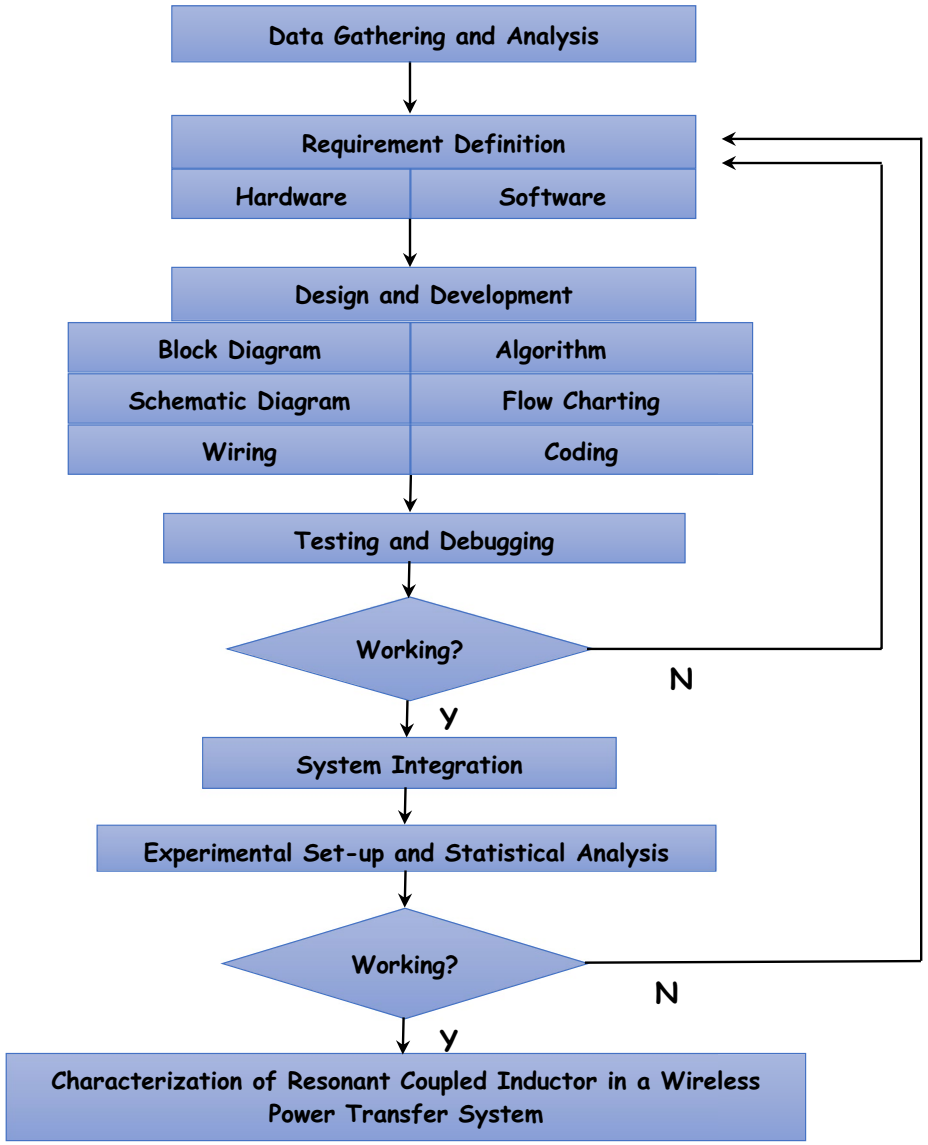

Fig. 1 Methodology flowchart

efficiency. The succeeding portions of the paper provide a full examination of these results, which provide a substantial contribution to the area of WPT.

In brief, the researcher carefully designed the approach to examine and validate the novel contributions of the study, so facilitating a comprehensive inquiry and notable progress in the domain of wireless power transmission.

Conceptualization/development of system design

System block diagram

The system, as depicted in Fig. 2, is structured into four main sections, all of which are essential for the overall functioning of the system. The initial component, known as the power amplifier, assumes a pivotal role within the system. The device is

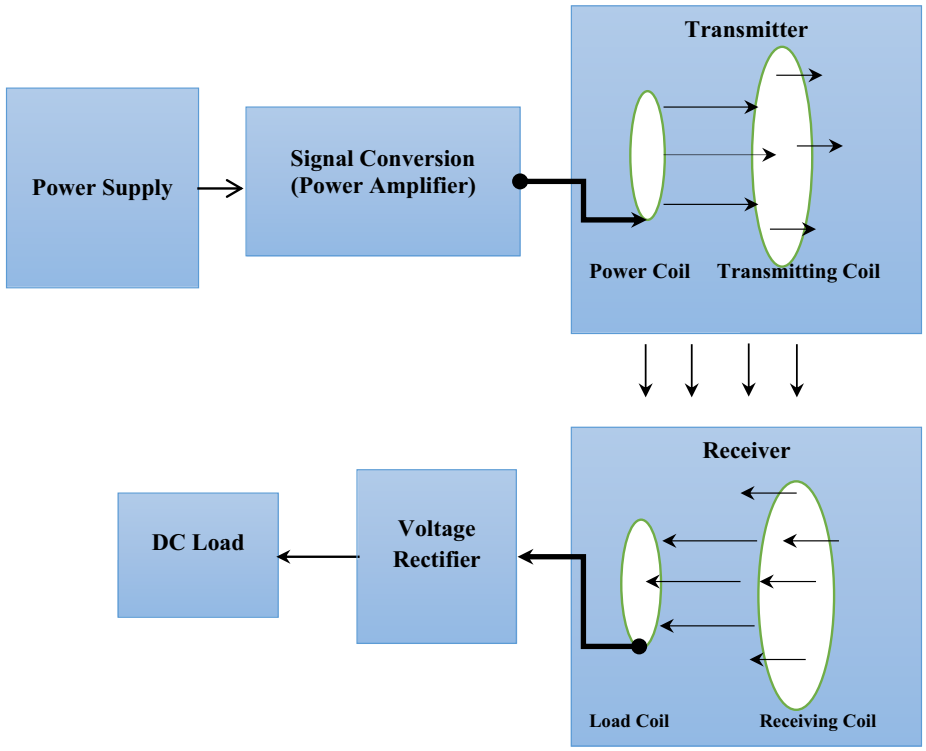

Fig. 2 The block diagram of the system

accountable for amplifying the power of the input signal. The radio frequency signal is amplified to a suitable level for transmission. The ability to adjust the output power allows for precise control over the desired signal strength, thereby playing a crucial role in optimizing the efficiency of wireless power transmission.

The subsequent section encompasses the transmitting loops, which serve as the primary antennas within the system. The primary purpose of power amplifiers is to transmit amplified signals into the surrounding environment. The amplified electrical signals are converted into electromagnetic waves that have the ability to propagate through space by the transmitting loops. The devices are intricately engineered to function at the resonant frequency of the system, thereby enabling efficient energy transfer.

The third section comprises the receiving loops, which function as the receiving antennas of the system. These devices have been designed to effectively capture electromagnetic waves emitted by transmitting loops and subsequently convert them into electrical signals. Like the transmitting loops, these devices are also specifically engineered to function at the resonant frequency of the system, thereby optimizing the absorption of energy from the electromagnetic waves being transmitted.

The last component of the system is the voltage rectifier, which is responsible for the conversion of the alternating current (AC) produced by the receiving loops into direct current (DC). Since a multitude of electronic devices require direct current (DC) for their functioning, the significance of this component becomes paramount in the context of implementing wireless power transmission in real-world scenarios.

Every component of the system has been meticulously crafted to align with the precise objectives of the study. Any alteration made to each individual section has the potential to directly impact the overall performance of the system, encompassing both efficiency and power transfer range. Hence, meticulous consideration is devoted to the design and implementation of each section, to guarantee that the overall system achieves optimal performance in accordance with the research objectives.

Amplifier

The amplifier's design in the wireless power transfer system has great importance, since it exerts a substantial impact on the overall performance of the system. The central element of this design is the metal–oxide–semiconductor field-effect transistor (MOSFET), a critical component that plays a pivotal role in the amplification process. The fundamental function of the amplifier is to increase the amplitude of an oscillating input signal, resulting in the production of a robust magnetic flux that efficiently generates a high voltage in the receiving loop. The enhancement of this amplification is of utmost importance for ensuring the smooth functioning of the wireless power transfer system.

The important characteristic of this amplifier design is the integration of a feedback loop originating from the transmitting antenna. The configuration described facilitates the redirection of the antenna's resonance frequency back into the amplifier, resulting in an amplified signal that is both improved and more stable. The use of this feedback mechanism plays a crucial role in enhancing the performance and efficiency of the system.

Circuit simulations were performed using Multisim software throughout the design and testing stages. Although the software's library did not have precise matches for the components used in the bench testing, appropriate generic alternatives were employed. By using this methodology, the simulations were effectively maintained with a high degree of accuracy and pertinence, so yielding significant insights into the behavior of the circuit, especially in relation to resonance and amplification.

The comprehension of the simulated circuit heavily relies on the schematic arrangement of the amplifier, as shown in Fig. 3. The tank circuit, which consists of components C1 and L3, replicates the impedance of the antenna load and is adjusted to achieve resonance at a frequency of 580 kHz. The establishment of this particular configuration is of utmost importance in order to effectively optimize the process of resonant energy transfer, which is a key objective of the present research endeavor.

Figure 4 offers significant insights into the operational characteristics of the amplifier as observed in the simulation. The tank circuit effectively generated oscillation, which is a vital component of the system's functioning. The oscillation was subsequently amplified via the MOSFET, thereby confirming the theoretical functionality of the amplifier.

Although the simulation had certain limitations arising from the utilization of generic components, it effectively demonstrated the fundamental operational principles of the amplifier. The obtained simulation results, as depicted in Fig. 4, demonstrate that the operating frequency closely approximates the desired value of 580 kHz. This observation suggests that the amplifier is effectively performing its intended function. The amplifier successfully operated, as evidenced by the achievement of an output voltage of approximately 36.7 V peak to peak.

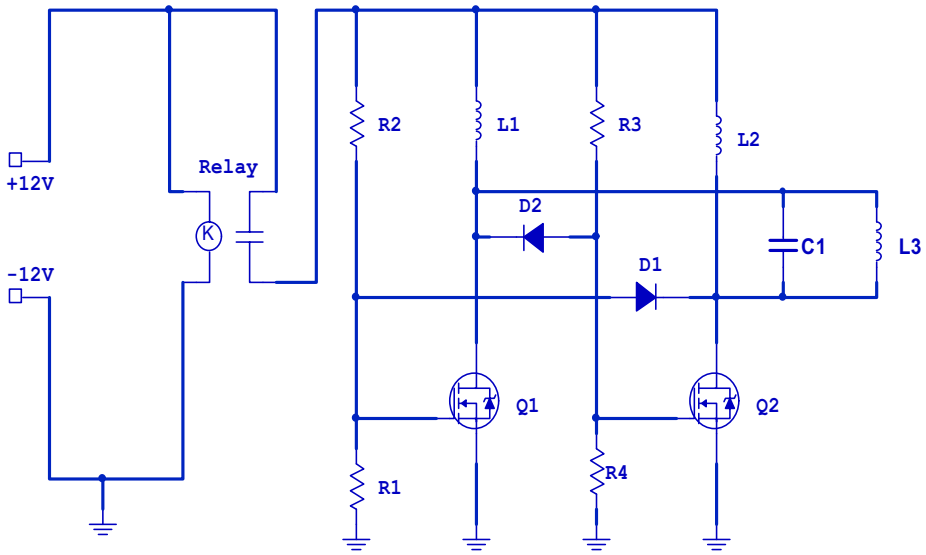

Fig. 3 Schematic diagram of amplifier

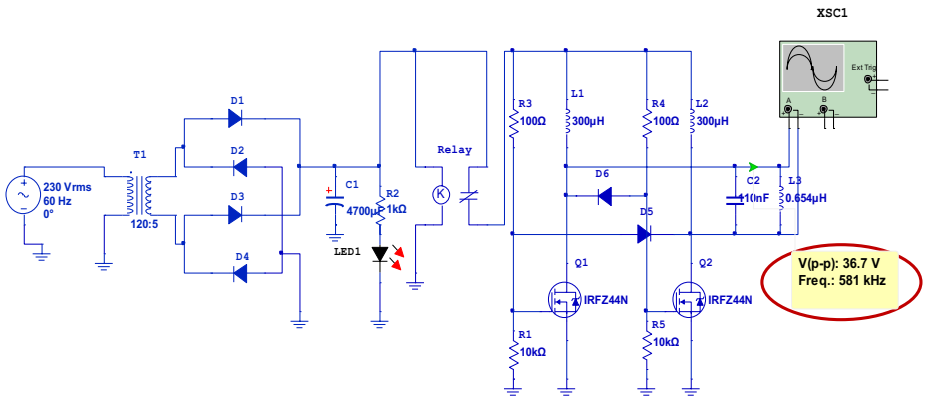

Fig. 4 Amplifier output in Multisim using measurement probe

The process of developing an amplifier for a wireless power transmission system entails the use of a series of mathematical equations that govern the system's performance attributes. The aforementioned equations play a pivotal role in guaranteeing the optimal functioning of the amplifier within the specified parameters. The fundamental design equations for a MOSFET amplifier used in wireless power transmission are as follows:

Voltage gain (AV)

$$A_v = -g_m\left(\frac{R_D R_L}{R_D + R_L}\right)$$

where g_m—the transconductance of the MOSFET, R_D—the drain resistance, and R_L—the load resistance

Transconductance (g_m)

$$g_m = \frac{2I_D}{V_{\mathrm{GS}} - V_{th}}$$

where I_D—the drain current, V_{GS}—the gate–source voltage, and V_{th}—the threshold voltage of the MOSFET

Input impedance (Z_{in})

In the case of a conventional source MOSFET amplifier, it is customary for the input impedance to exhibit a high value, mostly governed by the gate resistance, denoted as Rg.

$$\boldsymbol{Z}_{\mathrm{in}} = \boldsymbol{R_g}$$

Output impedance (Z_{out})

The drain resistance, Rd, plays an important part in determining the output impedance of the amplifier.

$$\boldsymbol{Z}_{\mathrm{out}} = \boldsymbol{R_d}$$

Drain current (I_d)

In the saturation region of the MOSFET operation,

$$\boldsymbol{I_d} = \frac{1}{2}\boldsymbol{k_n}\left(\boldsymbol{V}_{\mathrm{gs}} - \boldsymbol{V}_{\mathrm{th}}^2\right)$$

where k_n—the transconductance parameters of the MOSFET

Frequency response

The capacitance and resistance inside the circuit have an impact on the frequency response, particularly the cutoff frequency (fc).

$$\boldsymbol{f_c} = \frac{1}{2\boldsymbol{\pi}\mathrm{RC}}$$

In the given equation, the variables R and C denote the resistance and capacitance values inside the circuit, respectively.

Power dissipation (P_d)

$$\boldsymbol{P_d} = \boldsymbol{I_d}\boldsymbol{V}_{\mathrm{ds}}$$

where V_{ds}—the drain–source voltage.

Transmitter and receiver loops

The coupling circuit, comprising both the transmitter and receiver circuits, is the central component of the wireless power transfer system. This circuit is where the actual transfer of power wirelessly takes place, making it crucial to the overall functionality of the system. The efficiency of this coupling circuit is significantly influenced by the distance between the coils. To analyze this effect, the separation between the coils was made adjustable along their axis. Consequently, measurements were conducted across a direct current (DC) load at various distances. The outcomes of these measurements are systematically presented in Fig. 10.

The process of designing a resonator inside a wireless power transfer system encompasses a collection of essential equations that govern its resonant frequency and overall efficiency. The resonator is often comprised of an inductor and a capacitor, so establishing an LC circuit. The following equations are essential in the process of creating a resonator:

Resonant frequency (f_0)

The resonant frequency of the circuit obtained using the derived equation

$$f_0 = \frac{1}{2\pi\sqrt{LC}}$$

where $\boldsymbol{f_0}$, $\boldsymbol{L}$, and $\boldsymbol{C}$ are, respectively, the self-resonant frequency (***Hz***), equivalent capacitance (***F***), and inductance (μ***H***) of resonant circuit.

Quality factor

Coil Q-factor is counting by the classical formula, as the relation of its reactance to the active resistance:

$$\boldsymbol{Q} = \frac{\boldsymbol{X_L}}{\boldsymbol{R_L}} = \frac{2\pi \boldsymbol{fL}}{\boldsymbol{R_L}}$$

where Q—coil Q-factor (dimensionless value), X_L—coil reactance; Ohm, f—frequency; Hz, L—inductance; H, and R_L—common ohmic resistance of losses in the coil; Ohm

Reactance can be easily quantified, while active resistance poses more challenges in terms of measurement. This statement pertains to the cumulative losses incurred in a wire's ohmic resistance, skin effect, whirling currents (proximity effect), losses in the screen, the impact of nearby conductors, and the components of a structure exposed to the magnetic field of the coil. The influence of several factors on a coil's performance includes its self-capacitance, the choice of material and frame design, as well as the amount of wire smoothness. The aforementioned effects have a significant influence on the frequencies inside the RF range. However, within this frequency range, the operation is governed by the Q-factor principle, which mitigates the impact of losses.

Due to the inclusion of all losses, accurately quantifying the Q-factor becomes very challenging, rendering measurement a more feasible approach. However, it is feasible to create an approximate estimation of the Q-factor value for non-engineering uses and

amateur applications. In the software, the calculation of the active resistance of the one-layer coil is performed using the aforementioned formula.

$$R_L = \frac{k\sqrt{f}}{380d}\left[\sqrt{LD\left(102\frac{L}{D}+45\right)} + \frac{d^2\sqrt{L\left(102\frac{L}{D}+45\right)^3}}{50\left(\frac{L}{D}\right)^2\sqrt{D^5}}\right]$$

where d—diameter of a wire; mm, f—frequency; MHz L—inductance; μH, D—coil diameter (former diameter + wire diameter); mm, and k—correction factor considering a step between turns

$$k = \left(\cos^{-1} h\left(\frac{h}{d}\right)\right)^2$$

where h—step between turns; mm and d—diameter of a wire; mm

Active resistance of a single-turn loop is conducting by the formula:

$$R_L = 1.66x10^{-4}\frac{\pi D\sqrt{f}}{d}$$

where D—diameter of the loop; mm, d —diameter of a wire; mm, and f—frequency; MHz

The consideration of self-capacitance in the solenoid is not being accounted for. Hence, these computations are applicable for frequencies that are much lower than the self-resonant frequency of the solenoid.

Based on a rough estimation, it is not necessary to take into consideration the specific kind of wire material, such as copper or silver. However, it is evident that a coil constructed with silver wire would exhibit a higher Q-factor.

Inductor design using Coil32 v7.1

When constructing the inductor coil, it is crucial to consider many key characteristics, including the inductance (L), coil diameter, wire gauge, and the number of turns. The estimation of inductance may be accomplished by using the following method:

$$L = 2*D\left[\ln\frac{8D}{d} - 1.75\right]$$

The diameter of the loop is determined using the approach of gradual approximations. If the software displays the message "Coil cannot be realized" in the output text box, it indicates that the diameter of the loop is too big. In such cases, it is recommended to construct the coil as a one-layer coil, with each turn placed directly next to one another.

Voltage rectifier

The voltage rectifier is an essential element within the system. The device is tasked with the conversion of the received alternating current (AC) voltage from the load coil into a direct current (DC) voltage, thereby enabling its use for powering a DC load. The full-wave bridge rectifier has been selected as the preferred rectifying

circuit for this application due to its capability to produce an output voltage that is exclusively direct current (DC) or possesses a predetermined DC component. The rectifier in question employs a closed loop "bridge" configuration consisting of four interconnected rectifying diodes to achieve the intended output.

To mitigate the ripple present in the full-wave rectifier output, a smoothing capacitor is connected to the bridge circuit. The purpose of this arrangement is to convert the rippled output of the rectifier, which is a full-wave waveform, into a steady direct current (DC) voltage. This ensures a consistent and uninterrupted DC voltage supply for the load.

The selection of diodes for the rectifier holds significant importance in the design process, particularly when considering the rectification of high-frequency signals. The selection of fast signal diodes, specifically the 31DF4 type, for this system was based on their ability to efficiently rectify alternating current (AC) signals at frequencies in the megahertz range.

Circuit model and transfer system

The resonator system, illustrated in Fig. 5, can be understood by considering the lumped circuit components: L (inductor), C (capacitor), and R (resistor). The provided diagram depicts a circuit configuration that is well-suited for both manual analysis and SPICE simulations.

Figure 5 depicts a circuit diagram that is visually enhanced with illustrations. The diagram showcases the presence of four resonant circuits, which are interconnected through magnetic coupling coefficients denoted as k_{12}, k_{23}, and k_{34}. The power loop is energized by a source possessing a finite output impedance, denoted as R_S, commencing from the left. The power loop can be represented by a single-turn inductor, denoted as L_1, which is accompanied by a corresponding resistance, denoted as R_1. The inclusion of capacitor C_1 serves to establish resonance at the intended frequency within the power loop. The transmitter loop, denoted as T_x, consists of two components: the parasitic resistance R_2 and a single-turn air core inductor L_2. The self-capacitance, denoted as C_2, is determined by the geometry of the T_x loop. The inductors L_1 and L_2 are interconnected with a coupling coefficient k_{12}, and the receive side is defined in a similar manner. The interconnection between the transmitter and receiver loops is established through the coupling coefficient, denoted as k_{23}.

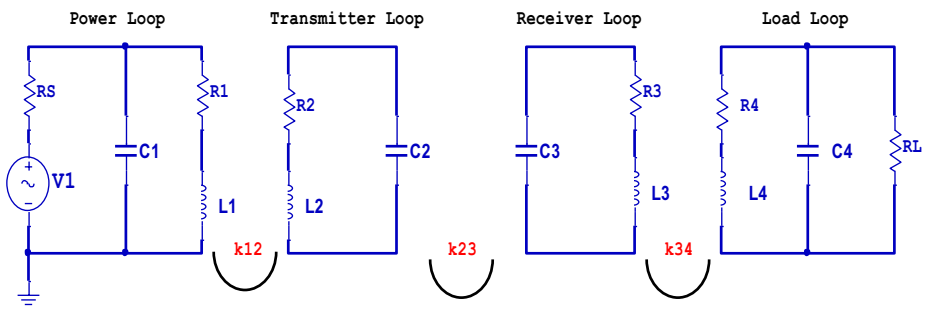

Fig. 5 Equivalent circuit model of the system

In a conventional implementation, the drive loop and the T_x coil would be combined into a unified entity, thereby resolving the issue of k_{12}. Similarly, the value of k_{34} would also remain constant. As a result, k_{23} would represent the sole uncontrolled variable, subject to variation depending on the distances separating the transmitting and receiving entities. The parallel resonators in the model represent each of the four antenna elements, which are interconnected by mutual inductances and coupling coefficients.

One effective approach for examining the transfer characteristics of a resonator system with magnetic coupling is to utilize the circuit model as a point of reference. To maintain simplicity in the analysis, the cross-coupling terms k_{12} and k_{34} are neglected. The circuit model provides a straightforward method for systematically examining the characteristics of the system. The utilization of Kirchhoff's voltage law (KVL) enables the representation of the connection between the current passing through each coil and the voltage applied to the power coil as illustrated in Eq. 1. This is achieved by determining the currents in each resonant circuit, as illustrated in Fig. 5. The coupling coefficient is defined by Eq. 2.

$$\begin{bmatrix} \boldsymbol{V_s} \\ 0 \\ 0 \\ 0 \end{bmatrix} = \begin{bmatrix} \boldsymbol{Z}_1 & \boldsymbol{j\omega M}_{12} & 0 & 0 \\ \boldsymbol{j\omega M}_{12} & \boldsymbol{Z}_2 & -\boldsymbol{j\omega M}_{23} & 0 \\ 0 & -\boldsymbol{j\omega M}_{23} & \boldsymbol{Z}_3 & \boldsymbol{j\omega M}_{34} \\ 0 & 0 & \boldsymbol{j\omega M}_{34} & \boldsymbol{Z}_4 \end{bmatrix} \begin{bmatrix} \boldsymbol{i}_1 \\ \boldsymbol{i}_2 \\ \boldsymbol{i}_3 \\ \boldsymbol{i}_4 \end{bmatrix} \tag{1}$$

$$\boldsymbol{k_{xy}} = \frac{\boldsymbol{M_{xy}}}{\sqrt{\boldsymbol{L_x L_y}}}, 0 \leq \boldsymbol{k_{xy}} \leq 1 \tag{2}$$

where V_s—voltage source. Z_1, Z_2, Z_3, and Z_4—loop impedance of the coil, M_{xy}, M_{12}, M_{23}, and M_{34}—mutual inductance between coils, i_1, i_2, i_3, and i_4—current in each coil, L_x and L_y—loop inductor, and k_{xy}—coupling coefficient between the coil

The symbol "M_{xy}" is used to represent the concept of mutual inductance between two coils, denoted as "x" and "y." Additionally, the symbols Z_1, Z_2, Z_3, and Z_4 are employed to represent the loop impedances of these four coils. The impedances are designated correspondingly.

$$\boldsymbol{Z}_1 = \boldsymbol{R_s} + \frac{\boldsymbol{R}_1 + \boldsymbol{j\omega L}_1}{\boldsymbol{\omega}^2\boldsymbol{L}_1 - \boldsymbol{j\omega C}_1\boldsymbol{R}_1 + 1} \tag{3}$$

$$\boldsymbol{Z}_2 = \boldsymbol{R}_2 + \boldsymbol{j}\left(\boldsymbol{\omega L}_2 - \frac{1}{\boldsymbol{\omega C}_2}\right) \tag{4}$$

$$\boldsymbol{Z}_3 = \boldsymbol{R}_3 + \boldsymbol{j}\left(\boldsymbol{\omega L}_3 - \frac{1}{\boldsymbol{\omega C}_3}\right) \tag{5}$$

$$\boldsymbol{Z}_4 = \boldsymbol{R_L} + \frac{\boldsymbol{R}_4 + \boldsymbol{j\omega L}_4}{\boldsymbol{\omega}^2\boldsymbol{L}_4 - \boldsymbol{j\omega C}_4\boldsymbol{R}_4 + 1} \tag{6}$$

where R_1, R_2, R_3, and R_4—internal resistance of each coil, R_s and R_L—resistance source resistance and load resistance, and C_1, C_2, C_3, and C_4—capacitance in each coil

The calculation of the current (i_4) in the load coil resonant circuit is determined by utilizing matrix in Eq. 1 through the application of the substitution method.

$$\boldsymbol{i_4 = -\frac{j\omega^3 M_{12} M_{23} M_{34} V_s}{Z_1 Z_2 Z_3 Z_4 + \omega^2 M_{12}^2 Z_3 Z_4 + \omega^2 M_{23}^2 Z_1 Z_4 + \omega^2 M_{34}^2 Z_1 Z_2 + \omega^4 M_{12}^2 M_{34}^2}} \quad (7)$$

The voltage across the load, denoted as V_L, can be expressed as -i_4 R_L, where i_4 represents the current flowing through the load, and R_L represents the load resistance. Additionally, a voltage-to-voltage relationship, denoted as V_L/V_s, exists between the source voltage (Vs) and the load voltage (V_L).

The system model bears resemblance to a two-port network. The S-parameter is a suitable metric for evaluating the efficiency of this system. The vector S_{21} quantifies the relationship between the signals leaving the output ports and the signals entering the input ports. The efficiency of power transfer is contingent upon the power gain, which is determined by the parameter $|S_{21}|^2$, representing the squared magnitude of S_{21}. The calculation of the S_{21} parameter is based on the work of Sample et al. [18], as referenced in the studies conducted by Fletcher and Rossing [5] and Mongia [13].

$$\boldsymbol{S_{21} = 2\frac{V_L}{V_S}\left(\frac{R_s}{R_L}\right)^{1/2}} \quad (8)$$

where S_{21}—system efficiency.

Therefore, by incorporating the equation $\boldsymbol{M_{xy} = k_{xy}\sqrt{L_x L_y}}$ derived from Eq. 2, the S_{21} parameter can be expressed as follows:

$$\boldsymbol{S_{21} = \frac{j2\omega^3 k_{12} k_{23} k_{34} L_2 L_3 \sqrt{L_1 L_4 R_s R_L}}{Z_1 Z_2 Z_3 Z_4 + k_{12}^2 L_1 L_2 Z_3 Z_4 \omega^2 + k_{23}^2 L_2 L_3 Z_1 Z_4 \omega^2 + k_{34}^2 L_3 L_4 Z_1 Z_2 \omega^2 + k_{12}^2 k_{34}^2 L_1 L_2 Z_3 Z_4 \omega^2}} \quad (9)$$

The utilization of Eq. 9 for the analysis of the system's performance proves to be advantageous. The efficiency of the system is determined by the parameter known as the magnitude of S_{21}. This parameter can be expressed as a function of two variables, namely, k_{23} and frequency. The values of all circuit parameters are found in Table 1. The coupling coefficient k_{23}, as previously mentioned, is the parameter that

Table 1 Component values in the circuit model

Parameter	Value
R_S, R_L	50Ω
L_1, L_4	0.654μH
C_1, C_4	110nF
R_1, R_4	0.20Ω
L_2, L_3	0.944μH
C_2, C_3	80nF
R_2, R_3	0.20Ω
k_{23}	0.001 to 0.30
f_o	580kHz
Frequency	100kHzto1.5MHz

undergoes changes in response to alterations in circumstances. The presence of a variable distance can result in variations in k_{23}. Moreover, alterations in the orientation or misalignment of the transmitting and receiving resonators have an impact on the coefficient. The mutual inductance between the coils exhibits a negative correlation with distance, implying that an increase in distance will result in an increase in the value of k_{23}. The k_{23} undergoes a modification when there is a variation in orientation or misalignment. The graphical representation in Fig. 6 illustrates the interconnections among S_{21}, k_{23}, and frequency. Based on the data presented in the figure, it can be observed that for scenarios, where k_{23} is small, such as instances involving significant separation between the transmitter and receiver or a combination of misalignment and orientation deviation, the efficiency, as indicated by the magnitude of S_{21}, exhibits a maximum value at the self-resonant frequency of approximately 580 kHz. Consequently, the resonant frequency undergoes variation in response to alterations in k_{23}.

A thorough analysis of the relationship between the magnitude of S_{21} and the variable k_{23} yields valuable insights. The magnitude of S_{21} exhibits a diminished value when the coefficient k_{23} assumes a significantly small value, a circumstance that arises when the distance between the transmitter and receiver is excessively large. The magnitude of $|S_{21}|$ exhibits an increase as the separation between the resonators decreases, which is attributed to an augmentation in the value of k_{23}. However, increasing the value of k_{23} does not necessarily lead to a higher magnitude of $|S_{21}|$ once the threshold level of $|S_{21}|$ is attained. Furthermore, a notable issue arises regarding frequency splitting, which substantially diminishes the efficiency of the apparatus. The location within the system at which the initial resonance frequency (593.383 kHz) deviates hold considerable influence. The superior performance of the system is evident through the relative positioning of the resonators. The efficiency is inadequately characterized when

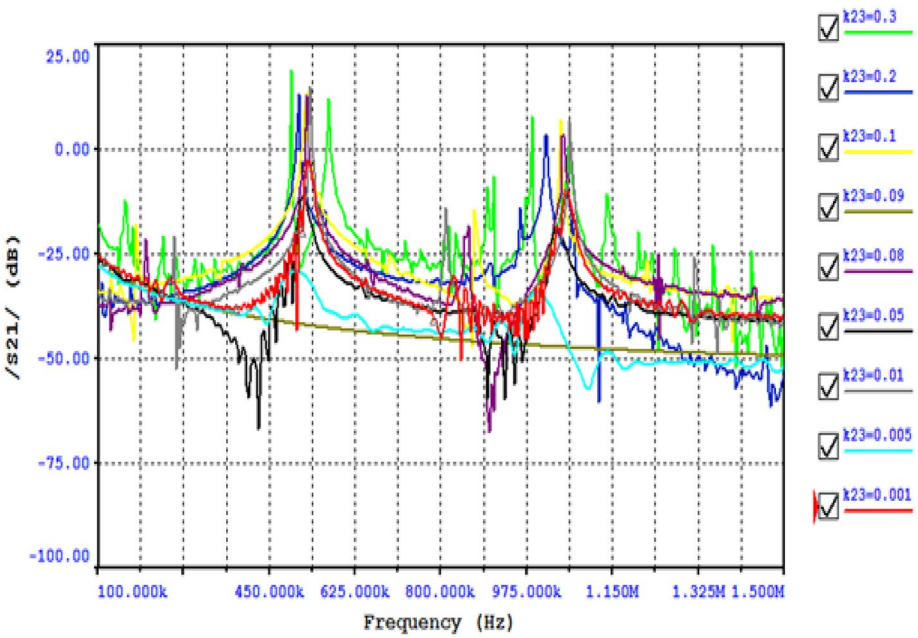

Fig. 6 $|S_{21}|$ as a function of k_{23} and frequency

the distance exceeds the specified range. However, the efficiency remains high despite the detuning of the resonant frequency in two furrows. Optimal power transmission would be achieved if the frequency could be adjusted to the desired frequency.

Experimental results and validation

This research expands upon the established framework for wireless energy transmission, with a specific emphasis on the utilization of inductive coupling between different components, as shown in Fig. 7. The practical configuration used in this study serves to confirm the proposed theoretical model. It comprises a transmitter on the left side, with a small driving loop and a bigger loop resonator. The resonator is precisely adjusted to a resonance frequency of 593.383 kHz, like the setups detailed in the work of Niculae et al. [15]. The recipient replicates this configuration, emphasizing the symmetrical nature of the design, which Cui et al. [2] identified as crucial for optimizing energy transmission.

The methodology for reliably calculating the lumped circuit parameters L, C, and R includes using well-established RF and microwave measurement technologies to handle the associated problems. This approach is consistent with the methodologies advocated by González-López et al. [6] in the extraction of essential characteristics from resonant structures.

One of the noteworthy facets of this study is in the capacity of this technology to promote the transfer of energy across different objects, a capability that has been acknowledged by Zhou, Liu, and Huang [22]. The experimental results obtained in this study indicate that the presence of non-metallic impediments, such as walls and organic glass, does not have a substantial impact on power transmission. This finding aligns with the findings drawn by Lee, Im, and Park [10].

The investigation conducted in this study about the impact of metallic items on energy transfer aligns with the conclusions made by Li and Huang [12]. The observation indicates that the influence of metallic items is dependent on their size and capacity to create eddy currents. The analysis of the interaction between metal objects and wireless energy systems is an important and complex field that warrants additional exploration, as shown by the research conducted by Huang et al. [7].

The outcomes of this study, as shown in Table 2 and Fig. 8, demonstrate a distinct negative correlation between voltage and the distance between the transmitter and receiver. This connection aligns with the observations made by Liu et al. [11]. The robustness of the linear regression model is supported by the substantial coefficient of determination (R^2), indicating a significant association between distance and voltage. This finding aligns

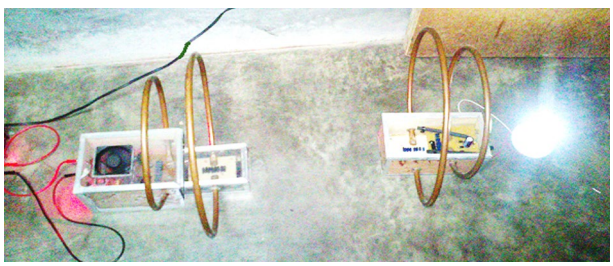

Fig. 7 The energy transfer experimental device

Table 2 Relationship between receiver output voltage and distance

Distance (cm)	Output voltage (Volts)	Distance (cm)	Output voltage (Volts)	Distance (cm)	Output voltage (Volts)	Distance (cm)	Output voltage (Volts)
0	10.83	30	8.09	60	2.73	90	0.603
5	10.15	35	7.04	65	2.07	95	0.469
10	9.79	40	6.29	70	1.57	100	0.345
15	9.68	45	5.43	75	1.212	105	0.246
20	9.45	50	4.83	80	0.975	110	0.006
25	9.24	55	3.58	85	0.742	115	0.007

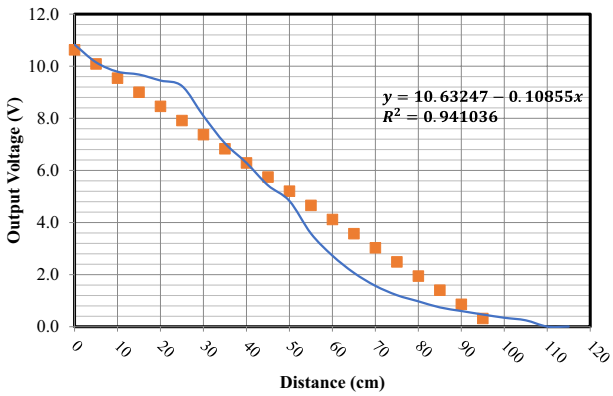

Fig. 8 Relationship between the transfer distance and output voltage of the load loop

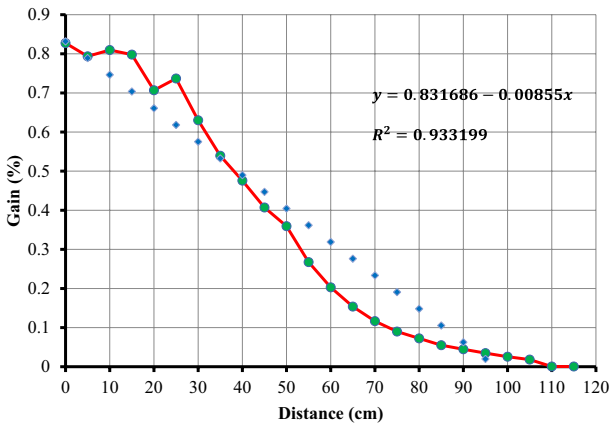

Fig. 9 Relationship between the voltage gain and the separation distance

with the observations made in the previous research conducted by Detka and Górecki [4].

In summary, this work serves to corroborate the results of other investigations while also contributing novel perspectives on the efficacy and feasibility of wireless energy transfer systems, specifically with regard to their ability to overcome obstacles and the impact of metallic objects.

Figure 9 illustrates a distinct correlation between the voltage gain and the spatial separation of the transmitting and receiving coils inside the wireless power transfer system. It can be noted that there is a direct relationship between coil separation and gain voltage, where the voltage gain grows as the distance between the coils decreases. The observed pattern aligns with the results obtained by Choi, Lee, and Park [1], who also documented a statistically significant association between the aforementioned factors. The graph shown in Fig. 9 serves to emphasize the influence of a limited distance between the coils. The statistical analysis conducted in this study, which includes the use of numerous R and R-square (R^2) values, serves to enhance the validity of this discovery. The R-square result, which indicates that 93.32 percent of the fluctuation in efficiency can be accounted for by the coil distance, is consistent with the findings of Choi, Lee, and Park. The study conducted by the authors sheds insight on the correlation between coil distance and voltage gain in wireless power systems, hence reinforcing the conclusions of our research. According to Choi, Lee, and Park [1], the significance of coil spacing in affecting the effectiveness of the system is emphasized.

System efficiency

When evaluating the efficiency of a system, the power transfer efficiency is determined by dividing the power received in the receiver coil by the power released from the transmitter coil, as described in Eq. 8. The results shown in Table 3 and depicted in Fig. 10 demonstrate a visible pattern: Enhanced efficiency is seen with decreasing distance between the transmitting and receiving coils. The graph, in addition to being of interest, demonstrates a discernible threshold for the distance between the coils. This barrier is shown by the point at which the zero-efficiency line intersects, implying the existence of an ideal range for coil spacing.

Table 3 Measured value for voltage, current, and power

Distance (cm)	Input			Output		
	Voltage (Volts)	Current (Ampere)	Power (Watts)	Voltage (Volts)	Current (Ampere)	Power (Watts)
0	5.61	7.72	43.3092	8.5	2.05	17.425
5	4.26	8.75	37.275	7.29	1.95	14.2155
10	11.48	2.75	31.57	4.54	1.6	7.264
15	12.63	1.94	24.5022	2.28	1.31	2.9868
20	12.68	1.85	23.458	1.79	0.52	0.9308
25	13.09	1.79	23.4311	1.72	0.31	0.5332
30	13.01	1.75	22.7675	1.702	0.18	0.30636
35	13.29	1.72	22.8588	1.67	0.11	0.1837
40	13.18	1.72	22.6696	1.645	0.07	0.11515
45	13.3	1.69	22.477	1.625	0.04	0.065
50	13.31	1.71	22.7601	1.59	0.02	0.0318
55	13.35	1.69	22.5615	1.5	0.01	0.015

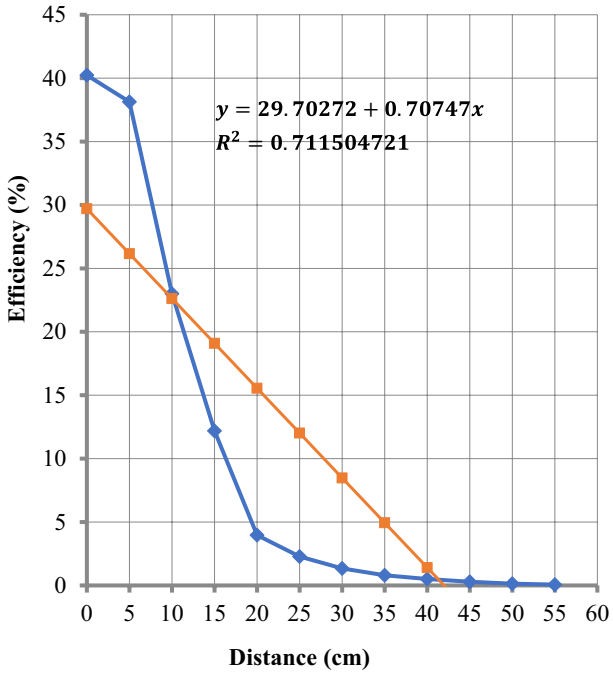

Fig. 10 Relationship between the transfer distance and system efficiency

The statistical analysis serves to further substantiate these findings. The coefficient of determination (R^2) indicates a robust link between the level of efficiency and the distance between coils. The *R*-squared (R^2) coefficient suggests that about 71.15% of the variability in measured efficiency can be explained by the variation in the distance between the coils observed in the experiment. Furthermore, a statistical examination of variance reveals an *F*-value of 24.66, which is statistically significant at a significance level of 0.01, with a p-value of 0.000564872. The findings of this study provide compelling evidence, indicating that the separation distance between the coils has a pivotal role in influencing the efficiency of our prototype.

The results found in this study are supported by recent research in the subject. The significance of coil distance in wireless power transfer efficiency has been underscored in studies conducted by Niculae et al. [15] as well as Okasili, Elkhateb, and Littler [16]. These investigations provide support for our results and add to a more comprehensive comprehension of the dynamics associated with wireless power transfer systems.

Voltage patterns as a function of angular displacements

The experimental configuration included a stationary generating coil and a moving receiving coil, as shown in Fig. 11. The receiving coil was rotated 360 degrees around the producing coil, while keeping a consistent distance between them. The radiation patterns obtained, as shown in Fig. 12, indicate that the energy emitted by the generating coil mostly disperses at a 90° angle in both the forward and backward directions relative to the coil. Significantly, the highest amounts of radiation were recorded at angular positions of 345° and 165°, which correspond precisely to the front and rear of the coil, respectively. The bidirectional pattern, which is controlled by the directivity of the coil,

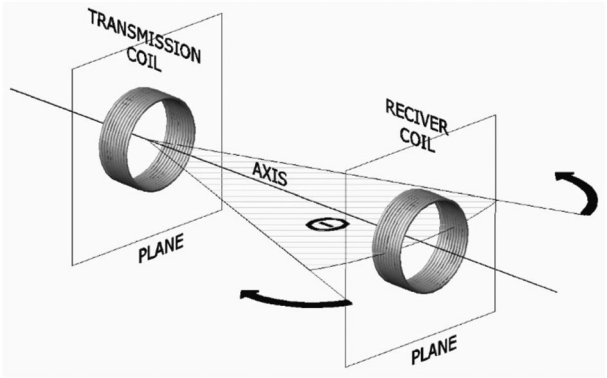

Fig. 11 Experimental process for the revolving coil

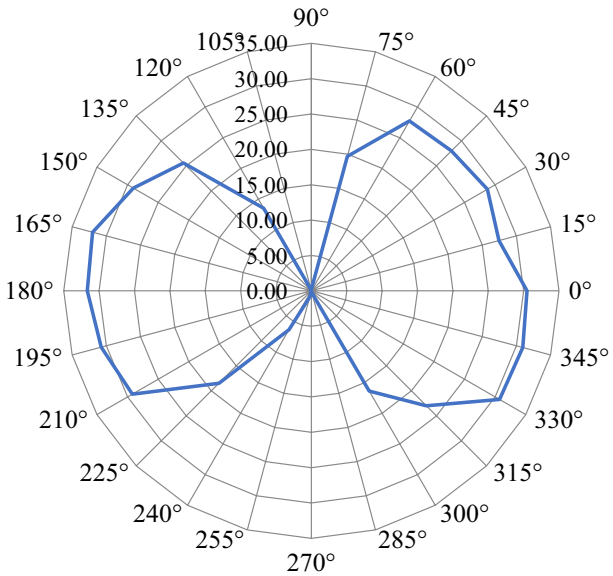

Fig. 12 Voltage pattern in different orientations

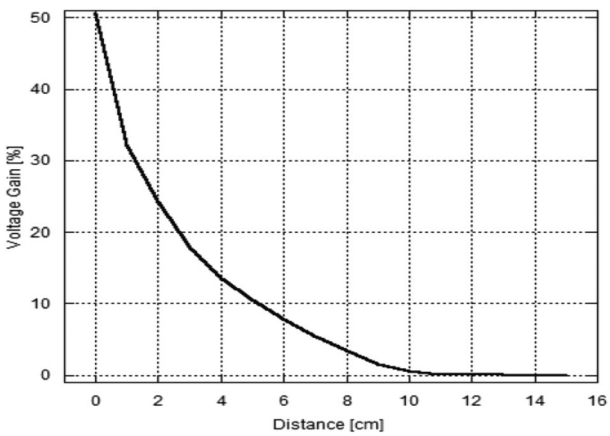

Fig. 13 System's voltage gain relative to voltage ratio

plays a significant role in the computation of the system's gain and overall efficiency. This phenomenon has also been seen in the research conducted by Yadav and Bera [21].

In order to assess the voltage gain, the receiving loop was systematically displaced from the stationary producing loop, and voltage measurements were recorded at each increment of displacement. The voltage ratios, as shown in Fig. 13, exhibit a discernible trend: Optimal energy transfer transpires precisely in front of the producing loop when the loops are in close proximity. This observation aligns with the radiation pattern shown in Fig. 12, especially in relation to the rear lobe, indicating a possible inefficiency in energy use. The voltage gain experiences a substantial decrease beyond a distance of 8 cm, as shown in Fig. 13, ultimately decreasing below 5%. This implies that the use of a surface capable of reflecting magnetic fields may have the ability to recover energy from the rear lobe, hence augmenting the efficiency of the system.

The aforementioned results align with the study done by Yadav and Bera [21], who similarly explored the effects of angular displacements on voltage patterns inside wireless energy transfer systems. The work presented by the authors offers further context and confirmation for our findings, namely, in elucidating the correlation between coil orientation, radiation patterns, and the efficacy of energy transfer.

Testing at different frequencies

The experimental data shown in Fig. 14 investigate the relationship between different driving frequencies, the resonant frequency, and the back electromotive force (EMF) on the load loop. The graph illustrates that variations in driving frequencies have a negligible effect on the amplitude. It is noteworthy that the resonant frequency remains unaffected by fluctuations in driving frequencies. The aforementioned observation plays a crucial role in comprehending the stability of the system across various operating settings.

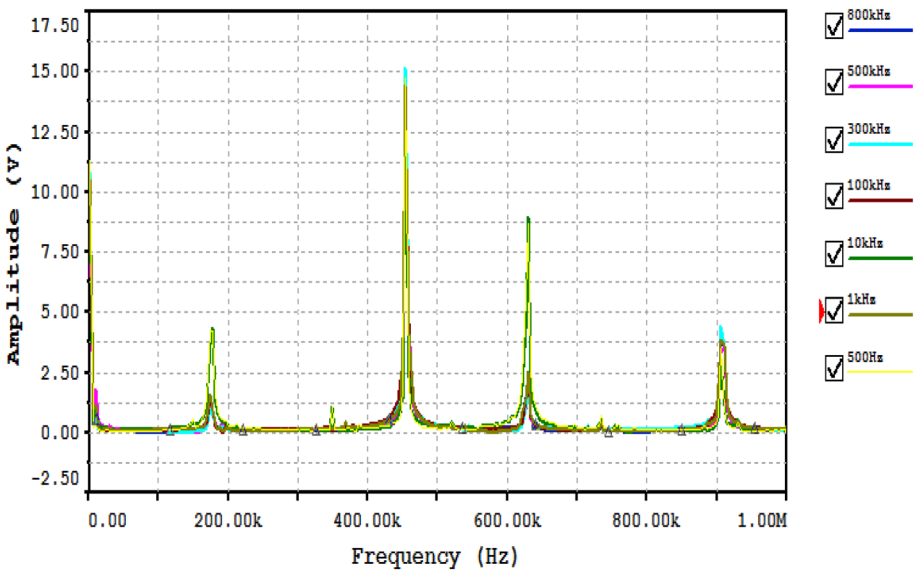

Fig. 14 Relationship between the different driving frequency, resonant frequency, and the output voltage on load loop

This phenomenon is consistent with the results reported by Pham et al. [17], who undertook an extensive investigation into the impacts of changes in driving frequency in comparable wireless power transfer systems. The study conducted by the researcher presents pertinent findings that align with our own observations on the consistency of resonant frequency in the face of changes in driving frequency. This research serves as a great framework for comprehending and analyzing our own results. The statement implies that certain wireless power transfer systems may exhibit intrinsic frequency stability properties, which might play a crucial role in the development of more efficient and dependable systems.

Conclusion

The present study investigating wireless energy transfer via magnetic resonance coupling has highlighted the significant prospects for advancement within this field. The research has provided evidence to support the notion that the transfer of electrical energy is optimized at the resonance frequency. This assertion has been validated by practical implementations using various devices such as a mobile phone, DC motor, LED, and bulb. The study revealed that the magnitude of the output voltage received in resonant wireless energy transfer is dependent upon the dimensions of the coil and the input voltage. Specifically, greater input voltages were seen to facilitate more efficient energy transfer. Furthermore, the dimensions and rate of incidence of the device are crucial considerations, since the resonance wireless energy transfer device functions within the medium- to high-frequency spectrum of the electromagnetic field.

This study establishes the fundamental principles for innovative wireless power technology, demonstrating the viability of using sophisticated electromagnetic resonance in wireless power transfer (WPT) systems for commercial use. The establishment of practicality has been achieved by the use of experimental data and analysis, wherein circuit simulations have been facilitated by the utilization of tools such as Multisim. The findings of this research demonstrate a prominent decrease in power transfer efficiency when considering distances outside the linked mode zone. These results support the prediction that efficiency diminishes as the distance between coil centers expands, with the most favorable efficiency seen at a distance of zero. The effectiveness of the coils is further impacted by the relative angles between their planes, with parallel alignment along the same axis being the most effective.

Subsequent research endeavors should prioritize the expansion of the aforementioned single-loop inductor circuit. The primary focal points include enhancing the efficiency at diverse distances, enhancing the stability and flexibility of the circuit under various operational conditions, and investigating novel materials and design methodologies to facilitate miniaturization and integration into a wider array of applications. Additional investigation might be conducted to explore sophisticated control methods for the purpose of dynamically adjusting parameters, as well as to examine the functioning of the circuit in intricate situations. By considering these issues, not only can the existing design be improved, but also the potential of wireless energy transfer technology will be broadened.

Acknowledgement
This study is the result of collaborative efforts and support from several people and organizations, for whom I express my heartfelt appreciation. First and foremost, I express my deep gratitude for the financial support given to me via the CHED scholarship program. This help has played a crucial role in enabling me to fulfill my academic responsibilities. Nueva Vizcaya State University warrants commendation for its dedication to provide high-quality education to the people of Nueva Vizcaya and adjacent provinces, helped by its initiatives in faculty and staff development. I would like to extend my sincere gratitude to Dr. Felicito S. Caluyo, the esteemed Dean of the College of Electrical Engineering and Computer Engineering (EECE) at Mapua Institute of Technology, for his invaluable mentorship, unwavering patience, and genuine concern, all of which significantly enhanced my educational journey during the course of this research endeavor. I would like to express my sincere gratitude to the esteemed members of the oral examination committee, namely Engr. Alejandro H. Ballado Jr., Engr. Marloun P. Sejera, and Engr. Marianne M. Sejera, for generously dedicating their time, sharing their important insights, and providing constructive criticisms that greatly enhanced the quality and accomplishment of this work. I would like to express my gratitude to Ms. Nancy Flores, the Dean of the College of Information Technology and Computer Sciences (CICTS)-UC, for her consistent support and encouragement. Additionally, I am appreciative to Dr. Juan V. Fontanilla Jr. for his significant contributions and presence. I would like to express my sincere appreciation to Dr. Aracelie V. Domagas, the Dean of the College of Engineering, for her invaluable assistance and understanding during the duration of my academic pursuits. I would like to express my gratitude to the academic members of the College of Engineering at NVSU-Bambang for their support and provision of essential resources over the course of this research endeavor. I express my gratitude towards Mr. James G. Bangunan for his valuable support and genuine interest. I would like to express my gratitude to the School of Graduate Studies, Dr. Jonathan W. L. Salvacion, and Ms. Rosie Ann Pascual for their unwavering support. I express my gratitude towards my immediate and extended family members, including my parents, mother-in-law, sisters-in-law, brothers, and sisters, for their steadfast and unwavering support throughout the demanding periods of my life. To my children, Lanj Anjelo and Lanj David, you serve as a profound source of inspiration and fortitude in my life, and I have a deep affection for you both. I express my profound gratitude to my spouse, Joan, for her unwavering encouragement and staunch support, which have proven to be of immeasurable value throughout periods of both prosperity and adversity. The affection you have bestowed upon me has served as a source of guidance, and my feelings for you are profound. Ultimately, I express my utmost admiration and appreciation to the divine being, God Almighty, who serves as the ultimate guiding force and perpetual wellspring of fortitude throughout this endeavor.

Author contributions
All the authors read and approved the final manuscript.

Funding
This research was not supported by any grant.

Data availability
The data that support the findings of this study are available from the Author, Alan P. Nebrida, Department of Electrical Engineering, Nueva Vizcaya State University, Bambang, Nueva Vizcaya, 3702 Philippines [DATA.docx.].

Declarations

Competing interests
The authors declare no conflicts of interest.

Received: 3 March 2023 Accepted: 30 December 2023
Published online: 24 January 2024

References

1. Choi Y-K, Lee D-J, Park S-J (2023) The effect of boost coil and alignment of transmitting and receiving coils on transmission efficiency in EV wireless power transfer systems. Energies 16(7):3213. https://doi.org/10.3390/en16073213
2. Cui H, Dong Z, Kim H-J, Li C, Chen W, Xu G, Qiu C-W, Ho J (2022) High-efficiency selective wireless power transfer with a bistable parity-time-symmetric circuit. Phys Rev Appl. https://doi.org/10.1103/PhysRevApplied.18.044076
3. Dionigi M, Costanzo A, Mongiardo M (2012) Network methods for analysis and design of resonant wireless power transfer systems. INTECH. https://doi.org/10.5772/25281
4. Detka K, Górecki K (2022) Wireless power transfer—a review. Energies 15(19):7236. https://doi.org/10.3390/en15197236
5. Fletcher R, Rossing T (1998) Principles of vibration and sound. Springer-Verlag, New York
6. González-López G, Jofre Roca L, García A, de Valdecasas S, Rodríguez-Leor O, Gálvez-Montón C, Bayés-Genís A, O'Callaghan J (2019) Resonance-based microwave technique for body implant sensing. Sensors 19(22):4828. https://doi.org/10.3390/s19224828
7. Huang Z, Zhou H, Zhang, & Ding. (2019) Effect of vertical metal plate on transfer efficiency of the wireless power transfer system. Energies 12(19):3790. https://doi.org/10.3390/en12193790
8. Komaru T, Koizumi M, Komurasaki K, Shibata T and Kano K (2012) Compact and tunable transmitter and receiver for magnetic resonance power transmission to mobile objects". In: Kim KY ed., Wireless power transfer—principles and engineering explorations, InTech, Rijeka, pp. 133–150. https://doi.org/10.5772/28068
9. Kurs A, Karalis A, Moffatt R, Joannopoulos JD, Fisher P, Soljačić M (2007) Wireless power transfer via strongly coupled magnetic resonances. Science 317(5834):83–86. https://doi.org/10.1126/science.1143254

10. Lee H-Y, Im S-H, Park G-S (2021) Effects of electro-magnetic properties of obstacles in magnetic resonant wireless power transfer. Energies 14(22):7469. https://doi.org/10.3390/en14227469
11. Liu C-Y, Wu C-C, Tang L-C, Shieh Y-T, Chieng W-H, Chang E-Y (2023) Resonant mechanism for a long-distance wireless power transfer using class E PA and GaN HEMT. Energies 16(9):3657. https://doi.org/10.3390/en16093657
12. Li J, Huang Y (2022) Influence analysis of metal foreign objects on the wireless power transmission system. Front Electron. https://doi.org/10.3389/felec.2022.1033016
13. Mongia R, Bahl IJ, Bhartia P, Hong SJ (2007) RF and microwave coupled-line circuits. Artech House Publishers. http://books.google.ie/books?id=XN5kQgAACAAJ&dq=RF+and+Microwave+Coupled-line+Circuits&hl=&cd=1&source=gbs_api
14. Nnamdi UC, Asianuba IB (2023) Wireless power transfer: a review of existing technologies. Eur J Eng Technol Res 8(3):59–66. https://doi.org/10.24018/ejeng.2023.8.3.3038
15. Niculae DM, Stanculescu M, Deleanu S, Iordache M, Bobaru L (2021) Wireless power transfer systems optimization using multiple magnetic couplings. Electronics 10(20):2463. https://doi.org/10.3390/electronics10202463
16. Okasili I, Elkhateb A, Littler T (2022) A review of wireless power transfer systems for electric vehicle battery charging with a focus on inductive coupling. Electronics 11(9):1355. https://doi.org/10.3390/electronics11091355
17. Pham TS, Nguyen T, Tung B, Khuyen B, Hoang T, Ngo QM, Hiep Le, Lam Vu (2021) Optimal frequency for magnetic resonant wireless power transfer in conducting medium. Sci Rep 11:18690. https://doi.org/10.1038/s41598-021-98153-y
18. Sample A P, Meyer D A, & Smith J R (2011) Analysis, experimental results, and range adaptation of magnetically coupled resonators for wireless power transfer". In: IEEE transactions on industrial electronics, vol. 58(2), pp. 544–554, Feb. 2011, doi: https://doi.org/10.1109/TIE.2010.2046002
19. Van Mulders J, Delabie D, Lecluyse C, Buyle C, Callebaut G, Van der Perre L, De Strycker L (2022) Wireless power transfer: systems, circuits, standards, and use cases. Sensors 22(15):5573. https://doi.org/10.3390/s22155573.PMID:35898075;PMCID:PMC9371050
20. Wei X, Wang Z, Dai H (2014) A critical review of wireless power transfer via strongly coupled magnetic resonances. Energies 7(7):4316–4341. https://doi.org/10.3390/en7074316
21. Yadav A, Bera TK (2023) Ferrite shielding thickness and its effect on electromagnetic parameters in wireless power transfer for electric vehicles (EVs). J Eng Appl Sci 70:132. https://doi.org/10.1186/s44147-023-00298-2
22. Zhou Y, Liu C, Huang Y (2020) Wireless power transfer for implanted medical application: a review. Energies 13(11):2837. https://doi.org/10.3390/en13112837
23. Zhang Y, Zhao Z, Li S (2018) A generalized power control algorithm for optimizing efficiency and load sharing in multi-coil wireless power transfer systems. IEEE Trans Power Electron 33(2):1507–1523. https://doi.org/10.1109/TPEL.2017.2698012

Publisher's Note